relaxation does match the EPR line width measured. The extrapolation of this situation to lower magnetic field strengths, however, is complex because eq 1 may be incorrect.[39,40] We report this simple approach because it does provide an estimate of the electronic contributions to the low magnetic field relaxation rates and may provide an indication of the dependence of the electron relaxation properties on the dynamical characteristics of the solution or when the complex is attached to a macromolecule. In this spirit, we note that, for both complexes, the electronic contributions to the correlation time increase with increasing viscosity, though the dependence is weaker even than that of the rotational correlation time.

In summary, the nuclear magnetic relaxation dispersion profiles for both the $Gd(DOTA)^-$ and $Gd(DTPA)^{2-}$ ions are described by a Lorentzian shape, which implies that an exponential correlation function is adequate to describe the fluctuations in the electron–nuclear coupling. Further, the high-field relaxation rate is dominated by the rotational motions in both complexes which are within experimental error the same. The high-field data have provided a direct measure of the rotational correlation times of the complexes as a function of solution viscosity that provides an opportunity to examine the low-field contributions by knowing the magnitude of the rotational correlation times. This analysis has provided an estimate of the electron spin-relaxation rates. The electron relaxation rates increase with increasing microdynamic viscosity, but not in the same proportion as the rotational correlation time. Thus, major changes in the dynamical environment of a paramagnetic metal center may not lead to significant changes in the efficiency of induced nuclear spin relaxation because of compensating changes in the contributions to the effective correlation time for the electron–nuclear coupling.

Acknowledgment. This work was supported by the National Institutes of Health (Grant GM39309), The University of Rochester, and the Squibb Institute for Medical Research. We also acknowledge the synthetic and analytical work of A. Krumwiede and S. C. Taylor.

(39) Bertini, I.; Luchinat, C.; Mancini, M.; Spina, G. *J. Magn. Reson.* **1984**, *59*, 213.
(40) Bertini, I.; Luchinat, C.; Kowalewski, J. *J. Magn. Reson.* **1985**, *62*, 235.

Contribution from the Departamento de Química, Faculdade de Ciências do Porto, 4000 Porto, Portugal

EPR and Electrochemical Study of Nickel(III) Complexes of Bis(3,5-dichlorosalicylaldehyde) *o*-Phenylenediimine. Evidence for Adduct Formation with Pyridines

Baltazar de Castro* and Cristina Freire

Received January 11, 1990

Electrochemical oxidation of [bis(3,5-dichlorosalicylaldehyde) *o*-phenylenediiminato]nickel(II), [Ni(3,5-Cl_2saloph)] (**1**), was performed in DMF and $(CH_3)_2SO$. In these strong donating solvents (S) the Ni(II) complex is oxidized to a Ni(III) complex (low-spin d^7 electron configuration), which can be formulated as $[Ni(3,5\text{-}Cl_2saloph)\cdot S_2]^+$. Upon addition by pyridines to freshly electrolyzed solutions of compound 1, novel electron paramagnetic resonance (EPR) spectra indicate the formation of new paramagnetic species, the species formed depending on the basic strength of the pyridines added. Thus, for the weaker bases, the EPR spectra indicate the presence of new Ni(III) species ($g_{av} \approx 2.12$) with the bases (B) coordinated axially ($[Ni(3,5\text{-}Cl_2saloph)\cdot B_2]^+$), whereas for the more strongly basic pyridines, the unpaired electron is transferred into the equatorial ligand, forming Ni(II) ligand radical complexes ($g = 2.00$). The analysis of the EPR parameters of Ni(III)–pyridine adducts suggests that the adducts have a d_{z^2} ($^2A_1$) ground state and also accounts for the observed g_z values, in excess relative to that of the free electron, as being due to the influence of low lying quartet states. The application of the same model to the analysis of the spin Hamiltonian parameters of the EPR spectra of $[Ni(3,5\text{-}Cl_2saloph)\cdot S_2]^+$, shows that it has a d_{z^2} ground state and yields values of $E(d_{xz},d_{yz} \rightarrow d_{z^2})$ in good agreement with those obtained from the electronic spectra.

Introduction

The recognition that the less-common oxidation states of nickel, Ni(III) and Ni(I), play a crucial role in the activity of several hydrogenases,[1a,b] of methyl coenzyme M reductase,[1c,d] and of carbon monoxide oxydoreductase (CO dehydrogenase)[1e,f] has spurred intense activity in the synthesis and characterization of Ni(III) and Ni(I) complexes.[1h] This activity has centered on the requirements for the stabilization of d^7 and d^9 electronic configurations for nickel and, particularly for complexes of the former, on factors that determine the relative stability of the Ni(III) complexes compared to Ni(II) radical complexes.[2]

There is accumulated evidence[3-5] that in the oxidation of Ni(II) square-planar complexes, where ligand-localized oxidation is also accessible, the final oxidation site (metal or ligand) depends on the ability of the solvent (or of other donors present in solution) to stabilize the high metal oxidation state through axial ligation. For macrocyclic or other π delocalized square-planar complexes, where the π energy levels of the ligand and those of the central Ni(II) ion are very similar, axial coordination can shift the d_{z^2} orbital above the filled ligand orbitals, thus making metal oxidation the preferred process. However in the absence of strong axial interactions, oxidation will probably result in the loss of an electron from the ligand-based π system.

Nickel(II) bis(salicylaldiimine) complexes provide good examples of systems where the oxidation potential of the ligands and of the complexes do not differ appreciably and where a large solvent dependence for the ultimate oxidation site is observed. In acetonitrile, and in other weak donor solvents (donocity number

(1) (a) Lancaster, J. R. *FEBS Lett.* **1980**, *115*, 285. (b) Albracht, S. P. J.; Graft, E.-G.; Thauer, R. K. *FEBS Lett.* **1982**, *140*, 311. (c) Gunsalus, R. P.; Wolfe, R. S. *FEMS Microbiol. Lett.* **1978**, *3*, 191. (d) Diekert, G.; Klee, B.; Thauer, R. K. *Arch. Microbiol.* **1980**, *124*, 103. (e) Pfaltz, A.; Juan, B.; Fässler, A.; Eschenmoser, A.; Jaenchen, R.; Gilles, H. H.; Diekert, G.; Thauer, R. R. K. *Helv. Chim. Acta* **1982**, *65*, 828. (f) Diekert, G.; Thauer, R. R. K. *J. Bacteriol.* **1978**, *136*, 597. (g) Diekert, G.; Graft, E.-G.; Thauer, R. R. K. *Arch. Microbiol.* **1979**, *122*, 117. (h) The bioinorganic aspects of nickel have been reviewed recently in *The Bioinorganic Chemistry of Nickel*; Lancaster, J. R., Jr., Ed.; VCH Publishers: New York, 1988.
(2) Lappin, A. G.; McAuley, A. *Adv. Inorg. Chem.* **1988**, *32*, 241.
(3) Kapturkiewicz, A.; Behr, B. *Inorg. Chim. Acta* **1983**, *69*, 247.
(4) Chavan, M. Y.; Meade, T. J.; Busch, D. H.; Kuwana, T. *Inorg. Chem.* **1986**, *25*, 314.
(5) Goldsby, K. A.; Blaho, J. K.; Hoferkamp, L. A. *Polyhedron* **1989**, *8*, 113.

0020-1669/90/1329-5113$02.50/0

smaller than that of acetonitrile DN = 14.1[6]), the electrochemical behavior of [Ni(salen)], [Ni(α,α'-Me_2salen)], and [Ni(saloph)] is complex; interpretations have been published that suggest ligand-centered oxidation followed by polymerization of the redox active species involving the phenolic portion of the salicylaldiimine chelate.[3,5] We have observed that, with the same systems [Ni(salen)], [Ni(α,α'-Me_2salen)], and [Ni(saloph)], in good donor solvent (DN $\gg$ 14.1), the Ni(II) complexes are oxidized to Ni(III) species.[7]

In the present study the oxidation of [Ni(3,5-Cl_2saloph)] (**1**) is performed electrochemically in strong donating solvents.

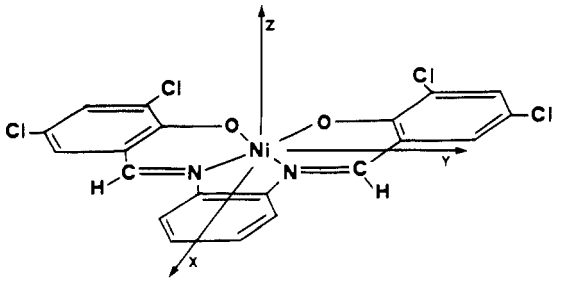

1

Electron paramagnetic resonance spectroscopy (EPR) is used to propose structures for the pyridine adducts of [Ni(3,5-Cl_2saloph)]$^+$ that are formed and to relate the strength of the axially coordinated bases with the relative stability of the Ni(III) complex when compared to Ni(II) radical complex. Previous reports in the literature claim that very strong bases favor decomposition of Ni(III) species;[8] we found that for the pyridines studied, those with the higher proton affinities are not able to stabilize Ni(III) species in solution. Nevertheless, the results of this study show that for axially coordinated pyridines (B) there is a narrow basicity range within which the species [Ni(3,5-Cl_2saloph)·B_2]$^+$ will be present in solution.

Experimental Section

Reagents, Solvents, Ligand, and Complexes. Pyridine and all solvents (Merck) were purified by using standard methods[9] and stored in the dark under nitrogen. All other bases (Aldrich) were used as received. The ligand 3,5-Cl_2saloph, bis(3,5-dichlorosalicylaldehyde) *o*-phenylenediimine,[10] the complex [Ni(3,5-Cl_2saloph)], bis[(3,5-dichlorosalicylaldehyde) *o*-phenylenediiminato)]nickel(II),[11] and tetraethylammonium perchlorate[12] were prepared by published procedures.

The oxidation of [Ni(3,5-Cl_2saloph)] was performed by constant potential electrolysis of its solutions in DMF/0.1 M TEAP at −10 °C or in $(CH_3)_2SO$/0.1 M TEAP at room temperature.

The adducts, prepared by addition of solutions or suspensions of the corresponding pyridines in toluene to a freshly electrolyzed solution of Ni(II), were immediately frozen in liquid nitrogen. Manipulations of Ni(III) species were carried out in a nitrogen atmosphere by use of standard Schlenk techniques or in a glovebox.

Abbreviations used: Me = methyl; Et = ethyl; py = pyridine; lut = lutidine; DMF = dimethylformamide; TEAP = tetraethylammonium perchlorate; saloph = bis(salicylaldehyde) *o*-phenylenediimine. Other abbreviations have their usual meaning.

Physical Measurements. Electrochemical measurements were performed with a VA-Detector E611, a VA-Scanner E 612, and a Coulometer E-524 (all from Metrohm). Cyclic voltammetry was performed in a three-electrode cell with a platinum microsphere as working electrode, a platinum wire as counter electrode, and a Ag/AgCl (1 M NaCl) reference electrode. In all cases ferrocene was added at the end of the experiment and used as an internal standard. All potentials are reported relative to the Ag/AgCl (1 M NaCl) reference electrode and to $E_{1/2}$ of the ferrocenium/ferrocene couple (Fc^+/Fc). Under the experimental conditions used (scan rate 50 mV s^{-1}) the potentials of the Fc^+/Fc couple are 500 mV in DMF and 480 mV in $(CH_3)_2SO$. Coulometry was carried out at controlled potential (about 50 mV more positive than the anodic peak potential) using a platinum gauze working electrode, a platinum foil as counter electrode, and a Ag/AgCl (1 M NaCl) reference electrode (all from Metrohm).

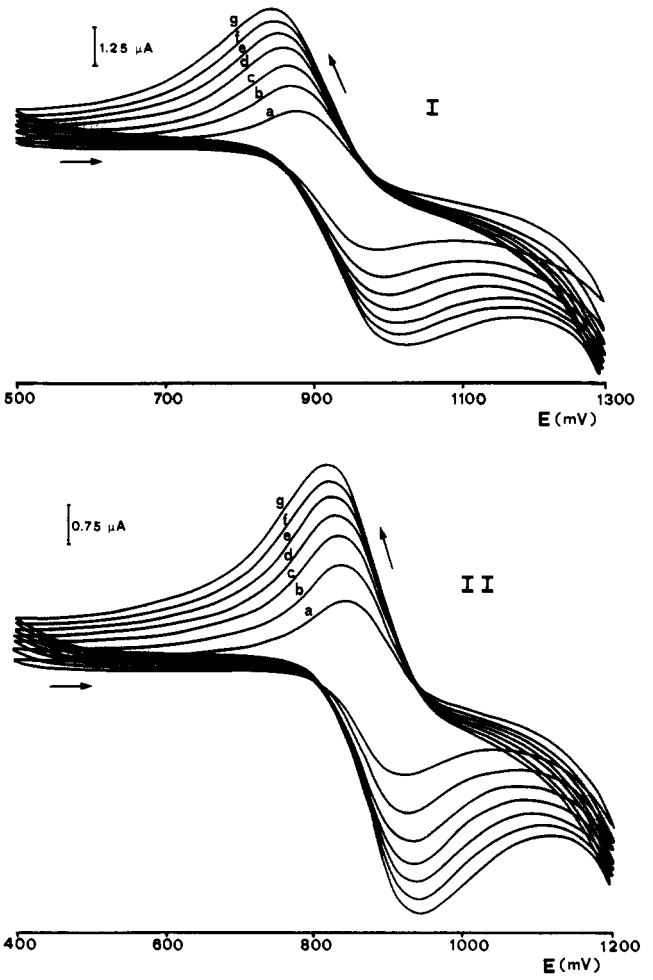

Figure 1. Variable-scan-rate cyclic voltammograms at 25 °C of [Ni(3,5-Cl_2saloph)] in (I) DMF/0.1 M TEAP and (II) DMSO/0.1 M TEAP; peak potentials vs Ag/AgCl (1 M NaCl) Scan rate (mV s^{-1}): (a) 10, (b) 20; (c) 30; (d) 40; (e) 50; (f) 60; (g) 70.

The high-performance liquid chromatography (HPLC) of the starting Ni(II) solution and of the oxidized solution after complete decay was performed with a Philips system (PU 4100 with UV–vis detector) using a Philips ODS 5 μ column.

EPR spectra were obtained with a X-band Varian E-109 spectrometer (9 GHz) equipped with a variable-temperature accessory. The spectra were calibrated with diphenylpicrylhydrazyl (dpph; g = 2.0037); the magnetic field was calibrated by use of Mn^{2+} in MgO. The spectra were recorded at −140 °C using sealed quartz tubes. The reported EPR parameters were obtained by computer simulation, in the usual manner.[13] The amplitudes of derivative EPR signals were used to estimate the concentration of paramagnetic Ni(III) centers in solution.[14]

The electronic spectra were recorded, at room temperature, with a Cary 17 DX spectrophotometer. Absorptivitiy coefficients were estimated by using the Ni(III) concentrations obtained from EPR spectra.

Results

Cyclic Voltammetry of [Ni(3,5-Cl_2saloph)]. Oxidation of the free ligand and of the nickel compound (**1**) was studied by cyclic voltammetry in DMF and $(CH_3)_2SO$ (Figure 1). Experiments were not performed in acetonitrile and in other poorly coordinating solvents, due to the limited solubility of [Ni(3,5-Cl_2saloph)] in them. The results for this compound and for [Ni(saloph)] are

(6) Gutmann, V. *The Donor-Acceptor Approach to Molecular Interactions*; Plenum: New York, 1978.
(7) de Castro, B.; Freire, C. Unpublished results.
(8) Barefield, E. K.; Mocella, M. T. *J. Am. Chem. Soc.* **1975**, *97*, 4238.
(9) Perrin, D. D.; Armarego, W. L. F.; Perrin, D. R. *Purification of Laboratory Chemicals*; Pergamon: Oxford, 1980.
(10) Chen, D.; Martell, A. E. *Inorg. Chem.* **1987**, *26*, 1026.
(11) Costa, G.; Puxeddu, A.; Reisenhofer, E. *J. Chem. Soc., Dalton Trans.* **1972**, 1519.
(12) Donald, S. T., Jr.; Julian, R. L. *Experimental Electrochemistry for Chemistry*; Wiley: New York, 1974.
(13) Pilbrow, J. R.; Winfield, M. E. *Mol. Phys.* **1973**, *25*, 1073.
(14) Poole, C. P., Jr. *Electron Spin Resonance*, 2nd ed.; Wiley: New York, 1983.

Table I. Cyclic Voltammetric Results for Saloph and 3,5-Cl_2saloph and Their Ni(II) Complexes in DMSO and DMF (0.1 M TEAP) at 25 °C[a]

	in DMF						in $(CH_3)_2CO$					
	Ag/AgCl (1 M NaCl)				Fc^+/Fc		Ag/AgCl (1 M NaCl)				Fc^+/Fc	
compound	E_{pa}	E_{pc}	ΔE	$E_{1/2}$	$E_{1/2}$	i_{pa}/i_{pc}[b]	E_{pa}	E_{pc}	ΔE	$E_{1/2}$	$E_{1/2}$	i_{pa}/i_{pc}
saloph	*c*						*c*					
3,5-Cl_2saloph	985	*d*					*c*					
Ni(saloph)	970	840	130	905	405		920	708	212	814	334	
Ni(3,5-Cl_2saloph)	1015	855	160	935	435	1[b]	938	828	110	883	403	1

[a] All potentials in mV. Solute concentration $\approx 10^{-3}$ M, 0.1 M TEAP; scan rate = 50 mV/s; $\Delta E = E_{pa} - E_{pc}$; $E_{1/2} = {}^1/_2(E_{pa} + E_{pc})$; and E_{pa} and E_{pc} are the anodic and cathodic peak potentials, respectively. Under the conditions used, $E_{1/2}(Fc^+/Fc)$ is 500 mV in DMF and 480 mV in $(CH_3)_2SO$. [b] The ratio was observed to change with scan rate, from 0.8 at 10 mV s^{-1} to 1.1 at 70 mV s^{-1}, but with values close to 1 for scan rates higher than 30 mV s^{-1}. The values of i_{pa} could not be determined very accurately since the anodic peak is partially superimposed on the that of the ligand. [c] The anodic peak was not observed in the range 0 to 1250 mV. [d] Irreversible.

summarized in Table I. In DMF, the ligand 3,5-Cl_2saloph shows an irreversible oxidation process at 985 mV, whereas in $(CH_3)_2SO$, no oxidation was observed within the potential range used.

In both solvents, the anodic–cathodic peak potential separation, in the cyclic voltammogram of compound **1**, is larger (105–160 mV; scan rate 50 mV s^{-1}) than expected theoretically for a one-electron reversible process;[15] however, under similar conditions the peak separation for the couple ferrocenium/ferrocene is 100 mV. With increasing scan rates a linear dependence is observed between E_p and i_p and between i_p and $v^{1/2}$.

The ratio i_{pc}/i_{pa}, on the other hand, is solvent dependent, being practically constant and equal to 1 in $(CH_3)_2SO$ for the scan rates studied (10–100 mV s^{-1}), whereas in DMF this ratio is scan rate dependent, only reaching values near 1 for scan rates higher than 30 mV s^{-1}. These latter values are subject to some uncertainty due to the close proximity of the oxidation peak of the ligand.

Oxidation of [Ni(3,5-Cl_2saloph)]. Electrochemical oxidation of [Ni(3,5-Cl_2saloph)] solutions in DMF and $(CH_3)_2SO$ produces a change in color from reddish to dark brown implying the formation of new species. The observation that room temperature (20 °C) EPR spectra of the oxidized complexes in DMF and $(CH_3)_2SO$ solutions exhibit a single broad line, with g_{iso} values of 2.175 and 2.168, respectively, strongly suggests a metal-centered oxidation process. At room temperature the oxidized complexes decay to EPR silent species in about 10 min in DMF and in 2 h in $(CH_3)_2SO$. The decay in DMF is significantly slower at −20 °C and the samples are stable in both solvents for a few days when frozen at liquid nitrogen temperature.

Frozen solution EPR spectra of the electrolytically synthesized nickel complexes (Figure 2a) show large **g** tensor anisotropy and are typical of low-spin $d^7(S = 1/2)$ electron configuration species, implying a formal oxidation of +3 for the nickel center. No superhyperfine splitting assignable to the equatorial nitrogens is observed. The new species in solution can be formulated as $[Ni(3,5\text{-}Cl_2saloph)\cdot S_2]^+$, where S represents a solvent molecule, since axial ligation with solvent molecules is expected for these species (see Discussion).

The time elapsed during the electrolysis in either solvent was never longer than 75 min, since after this period the formation of the oxidized species is slower than their decomposition, as can be observed by following the decrease in the intensity of the derivative EPR bands. The final concentration of the Ni(III) compound was estimated by EPR spectral analysis to be ca. 40% to 50% of the total nickel in solution.

In the absence of EPR crystal data for our complexes, the observed similarity between their **g** features and those of analogous cobalt(II) compounds[16] can be further extended to support the following orientation scheme for the tensor axes of the nickel complexes: $g_1 = g_x$; $g_2 = g_y$; $g_3 = g_z$, where g_1 and g_3 refer to the lowest and highest magnetic field g values, respectively. With this approach $g_x = 2.238$, $g_y = 2.204$, and $g_z = 2.023$ for the complex in DMF, and in $(CH_3)_2SO$ the **g** components are $g_x = 2.234$, $g_y = 2.204$, and $g_z = 2.020$ (Figure 2a).

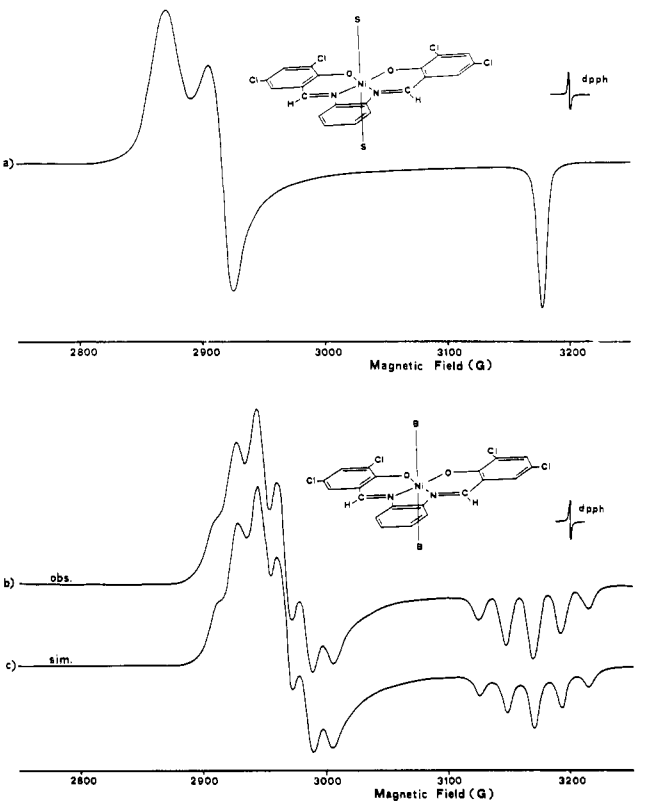

Figure 2. Frozen-solution (DMF/toluene) X-band EPR spectrum at −140 °C of (a) electrochemically oxidized solution of [Ni(3,5-Cl_2saloph)] and (b) electrochemically oxidized solution of [Ni(3,5-Cl_2saloph)] with 4-Me(py) and (c) computer simulation of spectrum b using the parameters in Table III and IV.

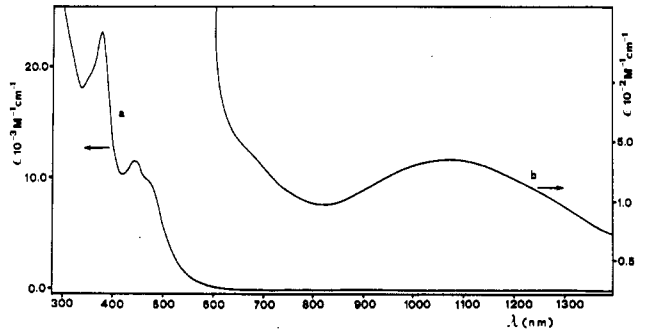

Figure 3. Near-IR/visible spectrum at 25 °C in DMSO/0.1 M TEAP of (a) [Ni(3,5-Cl_2saloph)] (4×10^{-5} M) and (b) electrochemically oxidized solution of [Ni(3,5-Cl_2saloph)] ($\approx 4 \times 10^{-4}$ M in Ni^{III}). The extinction coefficients for spectrum b can be in error by as much as 20% owing to the instability of the oxidized species and the process used to estimate the concentration of Ni^{III} centers in solution. (See text.)

The [Ni(3,5-Cl_2saloph)] electronic spectrum in $(CH_3)_2SO$ (Figure 3a) shows a weak band in the region 450–500 nm, the

(15) Bard, A. J.; Faulkner, L. R. *Electrochemical Methods, Fundamentals and Applications*; Wiley: New York, 1980.
(16) Daul, C.; Schlapfer, C. W.; von Zelewsky, A. *Struct. Bonding (Berlin)* **1979**, *36*, 129.

Table II. Pyridines Used to Form Adducts with Electrochemically Oxidized Solutions of [Ni(3,5-Clsaloph)], Type of EPR Spectrum Produced, and Proton Affinity

BASE	EPR signal[a]	PA[b]	BASE	EPR signal[a]	PA[b]
pyridine (py)	Ni(III) 1:2	924	3-NH_2py	radical	925
4-Me(py)	Ni(III) 1:2	942	2-Me(py)	Ni(III) 1:2	942
4-Et(py)	Ni(III) 1:2	940	2-Et(py)	radical	946
4-CNpy	Ni(III) 1:2	882[c]	2-CNpy	Ni(III) 1:2[c]	878[c]
4-HOpy	Ni(III) 1:2		2-Cl(py)	Ni(III) 1:2[b]	897
4-NH_2py	radical	961[c]	2-Br(py)	no signal[d]	898
4-Me_2Npy	radical	970[c]	2-HOpy	Ni(III)[f]	
3-Me(py)	Ni(III) 1:2	938	2-NH_2py	radical	936[c]
3-Et(py)	Ni(III) 1:2	937			
3-CNpy	Ni(III) 1:2	882[c]	2,6-Lut	radical	955
3-Cl(py)	Ni(III) 1:2	899	2,4-Lut	radical	951
3-Br(py)	Ni(III) 1:2	900	3,5-Lut	radical	943
3-HOpy	no signal[d]				

[a] Ni(III) 1:2 implies that [Ni(3,5-Cl_2saloph)·B_2]$^+$ must be present in solution and the resulting spectrum is similar to that depicted in Figure 2b; radical means that only a single line centered at $g = 2.00$ was observed. [b] Values in kJ mol^{-1}, taken from Lias, S. G.; Liebman, J. F.; Levin, P. D. *J. Phys. Chem. Ref. Data* **1984**, *13*, 695, unless otherwise stated. See this reference for the evaluation method used in the determination of the proton affinities and the associated experimental error limits. [c] Values adapted from Aue, D. H.; Webb, H. M.; Bowers, M. T.; Liotta, C. L.; Alexander, C. J.; Hopkins, H. P., Jr. *J. Am. Chem. Soc.* **1976**, *98*, 854, and corrected to be consistent with those of ref b. [d] No EPR signal was observed. [e] The EPR spectrum shows always superimposed on the signal of [Ni(3,5-Cl_2saloph)·B_2]$^+$ that of [Ni(3,5-Cl_2saloph)·S_2]$^+$. [f] The EPR signal obtained shows no superhyperfine structure and is similar to that of [Ni(3,5-Cl_2saloph)·S_2]$^+$.

solutions showing no absorption features at lower energies, as expected for low-spin Ni(II) planar species. Contrastingly, the room temperature electronic spectrum of the oxidized solution of compound **1** in $(CH_3)_2SO$ shows a very broad band in the near-IR region (λ = 1070 nm; ϵ = 420 M^{-1} cm^{-1}) and a higher energy band (λ = 650 nm; ϵ = 500 M^{-1} cm^{-1}) only discernible as a shoulder on a very intense absorption band (Figure 3b). These bands disappear, in what seems to be a first-order kinetic process in [Ni(III)], and the spectrum reverts to that of planar Ni(II) species.

The HPLC of pure solutions of [Ni(3,5-Cl_2saloph)] in DMF and in $(CH_3)_2SO$, when detected at either 270 or 560 nm, exhibit only a single peak which is assignable to the nickel compound. In contrast, the oxidized solutions of [Ni(3,5-Cl_2saloph)] after complete decay, show, in the same solvents, an additional peak at slightly smaller retention times.

Adduct Formation. On addition of pyridines (see Table II for list of pyridines used and their proton affinities) to freshly prepared solutions of [Ni(3,5-Cl_2saloph)·S_2]$^+$ in DMF, new paramagnetic species were formed as can be inferred from their novel EPR spectra, which can be classified into two broad groups.

In the first group, the spectra exhibit an EPR signal that is apparently isotropic and with a **g** value close to that of the free electron (g_e = 2.0023) as expected for metal–ligand radical species. Detailed analysis for these spectra is not presented, although we think that the signal can be assigned to radical species resulting from intramolecular electron transfer from the nickel center to the equatorial ligand as observed in other systems.[8]

In the second group, the observed **g**-tensor anisotropy and the values of $g_{av} \approx 2.12$–2.13 imply a metal-centered unpaired electron and a 3+ formal oxidation state for the metal. The observation of superhyperfine splittings in the three **g** regions, due to the interaction of the unpaired electron with nitrogen atoms, supports the assumption of axial coordination of the pyridines (Figure 2b).

Upon addition of base to [Ni(3,5-Cl_2saloph)·S_2]$^+$ in a molar ratio greater than 2:1, the EPR spectra of the resulting solutions show superhyperfine splittings, probably due to interaction of the unpaired with *two* equivalent nitrogens, yielding 1:3:5:3:1 quintuplets completely resolved in the z-region, with $a_z(N) \approx 22$ G, implying that these species can be formulated as [Ni(3,5-Cl_2saloph)·B_2]$^+$ (throughout this work 1 G = 10^{-4} T). On addition of pyridines to [Ni(3,5-Cl_2saloph)·S_2]$^+$ in a molar ratio less than 2:1, the EPR spectra of the resulting solutions are those of [Ni(3,5-Cl_2saloph)·S_2]$^+$ superimposed on that of [Ni(3,5-Cl_2saloph)·B_2]$^+$.

For all adducts, the spectral resolution in the x- and y-regions is insufficient to allow full observation of the multiplets [$a_{x,y}(N) \approx 14.0$–17.0 G]. The **g** and N coupling constants for the spectra of all these species, obtained by computer simulation, are presented in Tables III and IV.

Discussion

Cyclic Voltammetry of [Ni(3,5-Cl_2saloph)]. In $(CH_3)_2SO$ the complex is oxidized in a process that closely resembles reversible charge transfer. At 50 mV s^{-1} ΔE_p = 105 mV ($\Delta E_p(Fc^+/Fc)$ = 100 mV) and increases slightly with scan rate; $i_p/v^{1/2}$ is independent of scan rate, and $i_{pc}/i_{pa} \approx 1$. These results also provide support for chemical reversibility within the cyclic voltammetric time scale.

The results in DMF show a different behavior and the claim for chemical and electrochemical reversibility cannot easily be supported despite the independence of the ratio $i_p/v^{1/2}$ on scan rate, since ΔE_p = 160 mV at 50 mV s^{-1} and i_{pc}/i_{pa} approaches 1 only for scan rates higher than 30 mV s^{-1}. A possible explanation for these observations may lie in the possibility that the oxidized species have reduction paths other than that associated with one electron transfer involving the metal center.

Similarly, the HPLC results suggest that the oxidized solution must partially decay to different nickel(II) complexes. The observation, in both solvents, of a new peak near that of compound **1** in the chromatogram of the oxidized solution after complete decay supports the assumption that new species exist in the solution; the fact that the peak area ratio, between the new peak and that of compound **1**, is higher in DMF can be considered confirmation of the importance of other paths in the decomposition of Ni(III) compounds in this solvent.

The observation that the anodic peak potentials shift to less positive values in the stronger donating solvent ($(CH_3)_2SO$) also implies that an important role in the stabilization of the Ni(III) formal oxidation states is to be expected from axial coordination

Table III. EPR Parameters for [Ni(3,5-Cl_2saloph)·B_2]$^+$ Complexes

							coefficients[b]			energy transitions/cm^{-1}		
base	g_x	g_y	g_z	$(g_x + g_y)/2$	g_{av}[a]	$g_x - g_y$	C_1	C_2	C_3	$E(xz \rightarrow z^2)$	$E(yz \rightarrow z^2)$	ΔQ[c]
py	2.180	2.160	2.025	2.170	2.122	0.020	0.023	0.026	0.111	15610	13700	3240
4-Me(py)	2.187	2.170	2.027	2.178	2.128	0.017	0.024	0.027	0.116	14810	13300	3070
4-Et(py)	2.178	2.159	2.027	2.168	2.121	0.019	0.022	0.025	0.114	15890	14030	3130
4-CNpy	2.189	2.167	2.026	2.178	2.127	0.022	0.024	0.028	0.113	14930	12990	3170
4-HOpy	2.184	2.167	2.026	2.176	2.126	0.017	0.024	0.027	0.113	14950	13390	3180
3-Me(py)	2.179	2.159	2.025	2.169	2.121	0.020	0.023	0.026	0.115	15820	13830	3200
3-Et(py)	2.178	2.160	2.026	2.169	2.121	0.018	0.023	0.026	0.112	15750	13970	3190
3-CNpy	2.203	2.170	2.024	2.187	2.132	0.022	0.025	0.030	0.110	14470	11900	3240
3-Cl(py)	2.188	2.166	2.024	2.177	2.126	0.022	0.024	0.028	0.110	14910	12980	3260
3-Br(py)	2.189	2.166	2.024	2.178	2.126	0.023	0.024	0.028	0.110	14910	12900	3260
2-Me(py)	2.178	2.159	2.026	2.169	2.121	0.019	0.023	0.026	0.112	15830	13930	3190

[a] See ref 22. [b] Obtained from the resolution of McGarvey equations. [c] ΔQ is the difference between the average energy of the quartet states and the ground state.

Table IV. Nitrogen-14 Superhyperfine Coupling Constants and Spin Densities for $[Ni(3,5\text{-}Cl_2saloph)\cdot B_2]^+$ Complexes[a]

	experimental superhyperfine coupling					anisotropic superhyperfine tensor		spin densities on ^{14}N			
base	A_x	A_y	A_z	$(A_x + A_y)/2$	A_{iso}[b]	$A_{xx,yy}$	A_{zz}	C_{2s}^2	C_{2p}^2	total,[c] %	λ^2
py	16.2	17.8	22.5	17.0	18.8	−1.8	3.6	0.034	0.107	28.2	3.2
4-Me(py)	17.5	17.7	22.5	17.6	19.2	−1.6	3.1	0.034	0.099	25.4	2.7
4-Et(py)	17.5	17.5	22.5	17.5	19.4	−1.6	3.2	0.034	0.096	26.0	2.8
4-CNpy	16.2	17.2	22.5	16.7	18.4	−1.9	3.8	0.033	0.113	29.2	3.4
4-HOpy	17.7	17.7	22.5	17.7	19.3	−1.6	3.1	0.035	0.093	25.6	2.7
3-Me(py)	16.9	17.5	22.5	17.2	19.0	−1.7	3.4	0.034	0.101	27.0	3.0
3-Et(py)	17.1	17.3	22.5	17.2	19.0	−1.7	3.4	0.034	0.101	27.0	3.0
3-CNpy	15.9	15.7	22.2	15.8	17.9	−2.0	4.2	0.032	0.125	31.5	3.9
3-Cl(py)	16.3	17.1	22.5	16.7	18.6	−2.0	3.8	0.033	0.113	29.2	3.4
3-Br(py)	15.0	15.7	21.4	15.4	17.4	−2.0	4.0	0.031	0.116	29.4	3.7
2-Me(py)	17.4	17.4	22.5	17.4	19.1	−1.6	3.3	0.034	0.099	26.6	2.9

[a] The A values are expressed in gauss. [b] A_{iso} could not be obtained for the adducts and A_{av} values are used instead, with $\langle A_{iso}\rangle = {}^1/_3(2A_\perp + A_\parallel)$, where $A_\parallel = A_z$ and $A_\perp = {}^1/_2(A_x + A_y)$, since axial symmetry for the nitrogen coupling tensor was assumed as $A_x \approx A_y$. [c] Spin density delocalized into the two axial nitrogen atoms.

of the solvent. The EPR parameters (see below) also support this assumption.

The Ni(II)/Ni(III) oxidation potential for $[Ni(3,5\text{-}Cl_2saloph)]$ is higher than that observed for Ni(II)(saloph)/Ni(III)(saloph), which implies that the Cl groups directly affect the electron density on the metal throughout the delocalized chelate ring. With these electron-withdrawing groups in the phenol part of the ligand, less electron density resides on the chelate ring, which would result in less electron density on the central metal atom; consequently the d_{z^2} orbital would be less antibonding in 3,5-Cl_2saloph complex than in the saloph complex.

Electronic Spectra. The spectra of the oxidized solutions of compound **1** are similar to those of other Ni(III) complexes.[17-20] The band assignment was made assuming that the high intensity band in the visible region is probably due to fully allowed, ligand to Ni(III) charge transfer (LMCT) transitions and, in our case, also to the presence of Ni(II) species. Since the spectra of the latter compounds, as well as those of the oxidized solutions after complete decay, do not show any band at wavelengths longer than 600 nm, the two low intensity bands ($\epsilon \approx 400$–500 M^{-1} cm^{-1}) can be assigned to spin and symmetry allowed Ni(III) d–d transitions.

However, an unambiguous assignment has yet to be made for similar hexacoordinated complexes of Ni(III), but some insight can be gathered from the single crystal, visible absorption spectrum of $[Ni(dp)_2Cl_2]PF_6$, where dp = *o*-phenylenebis(dimethylphosphine).[18a] The observed bands for this complex are in good agreement with the transition energies calculated for the complex, assuming a 25% reduction in the values of interelectronic repulsion integrals and accepting the d-orbital ordering of $xy > z^2 > xz > yz > x^2 - y^2$. This ordering was also obtained for $NiCl_2$-(DOHDOpn), by semiempirical calculations,[17] using the referential depicted in the drawing of compound **1**. The assignment provided for $[Ni(dp)_2Cl_2]PF_6$,[18a] allows for the possibility of the following interpretation of our spectra, the band at 650 nm (15 400 cm^{-1}) corresponding to the $z^2 \rightarrow xy$ transition and the broad band at 1070 nm (9350 cm^{-1}) decomposing into two transitions at $\approx$ 10 200 and 8700 cm^{-1}, associated with the $xz \rightarrow z^2$ and the $yz \rightarrow z^2$ electronic transitions.[18b]

EPR Spectra Analysis of Ni(III) Complexes. g Tensor. Frozen solution EPR spectra of the oxidized solutions of compound **1** and of some of their base adducts show substantial **g** tensor anisotropy (rhombic symmetry) and have g_{av}[21] values in the range 2.12–2.16. This clearly indicates a metal-centered unpaired electron, which, for nickel, must be associated with the d^7 low-spin electron configuration expected for a 3+ formal oxidation state of the metal.

The absence of superhyperfine splitting in the EPR spectra of the oxidized solutions of **1** and the appearance of superhyperfine splitting due to nitrogen atoms in the adducts suggest the coupling to be due to the axially bound pyridines, thus supporting the existence, in solution, of hexacoordinate complexes. The observation $g_z < g_x, g_y$ implies axial elongation along the z axis, leading to a $C_{2v}(x)$ molecular symmetry, as would be expected for an almost planar tetracoordinate N_2O_2 ligand.

The larger splitting observed in the g_z component of $[Ni(3,5\text{-}Cl_2saloph)\cdot B_2]^+$, suggests that the unpaired electron lies in an orbital that is mainly d_{z^2} in character, implying a $^2A_1$ ground state ($a(d_{z^2} + b(d_{x^2-y^2})$, assuming a mixture of d_{z^2} and $d_{x^2-y^2}$ allowed in this symmetry, with $a \gg b$). Although no superhyperfine splitting can be observed in the EPR spectra of $[Ni(3,5\text{-}Cl_2saloph)\cdot S_2]^+$ with the coordinated solvent atoms (^{16}O has nonmagnetic nuclei), the same ground state is assumed since the pattern of g values is very similar.

The lack of superhyperfine splittings due to the in-plane nitrogen atoms has also been observed in analogous cobalt compounds with a $(d_{z^2})^1$ electronic configuration.[23,24] This behavior has been interpreted as to imply very little spin delocalization through σ bonding from the x and y components of the d_{x^2} orbital and delocalization of unpaired spin density by way of π bonding throughout the ligand π system and not concentrated on the nitrogen atoms.[23,24] This explanation has also been used to account for the lack of coupling with equatorial nitrogens in $[NiX_2(DO-DOHpn)]$[17] and $[NiX_2(cyclam)]^+$[25], where very little spin delocalization takes place in the plane of the "macrocyclic" ligand.

(17) Bemtgen, J. M.; Gimpert, H. R.; von Zelewsky, A. *Inorg. Chem.* **1983**, *22*, 3576.
(18) (a) Chandramouli, G. V. R.; Manoharan, P. T. *Inorg. Chem.* **1987**, *26*, 3291. (b) It must be pointed out that the symmetry of $[Ni(dp)_2Cl_2]PF_6$ is D_{2h} whereas that of $[Ni(3,5\text{-}Cl_2saloph)\cdot S_2]^+$ is C_{2v}. Nevertheless, with the choice of axis used in the treatment of the electronic data on the latter complex [see drawing of compound **1**; the symmetry is $C_{2v}(x)$], the ordering of the energy of the d orbitals is identical for both complexes.[17,18a] Furthermore, the reduction in symmetry from D_{2h} to C_{2v} does not affect the ordering of the states, thus enabling the use of the band assignment presented for $[Ni(dp)_2Cl_2]PF_6$.
(19) Kirvan, G. E.; Margerum, D. W. *Inorg. Chem.* **1985**, *24*, 3245.
(20) Mehne, L. F.; Wayland, B. B. *Inorg. Chem.* **1975**, *14*, 881.
(21) The g_{iso} values of the oxidized complex in DMF show a strong temperature dependence and level off at ca. 0 °C to a value that is larger than that of g_{av}. This last observation, also observed in DMSO, has also been found for aqueous solutions of electrochemically generated Ni(III) peptide compounds, where the values of g_{iso} are consistently larger by 0.01 than those of g_{av} for the glassy state.[22] The fact that pure solutions of Ni(III) compounds in CH_2Cl_2 do not exhibit this behavior[17] supports the suggestion that the difference in g values may be due to a change in the surrounding environment of the metal complex.[22b] Also, since the adducts are not stable in fluid solutions, no experimental values for g_{iso} could be obtained. Accordingly, in all subsequent discussions values of g_{av} were used, with $\langle g_{av}\rangle = {}^1/_3(g_x + g_y + g_z)$.
(22) (a) Subak, E. J., Jr.; Loyola, V. M.; Margerum, D. W. *Inorg. Chem.* **1985**, *24*, 4350. (b) Pappenhagen, T. L.; Kennedy, W. R.; Bowers, C. P.; Margerum, D. W. *Inorg. Chem.* **1985**, *24*, 4356.
(23) (a) Labauze, G.; Raynor, J. B. *J. Chem. Soc., Dalton Trans.* **1980**, 2388. (b) Labauze, G.; Raynor, J. B. *J. Chem. Soc., Dalton Trans.* **1981**, 590.
(24) Pezeshk, A.; Greenaway, F. T.; Dabrowiak, J. C.; Vincow, G. *Inorg. Chem.* **1978**, *17*, 1717.
(25) Desideri, A.; Raynor, J. B.; Poon, C. K. *J. Chem. Soc., Dalton Trans.* **1977**, 2051.

We assume that a similar explanation will hold for our complexes, corroborating the previous assumption of a ground state that is essentially d_{z^2}.

The observed g_z values, as in the EPR spectra of other Ni(III) complexes,[17,19,20,22,25] do not fit Maki's equations based on second-order perturbation theory[26] that predicts $g_z = g_e = 2.0023$. Similar behavior is observed for analogous Co(II) compounds for which McGarvey developed a model that includes the contribution of low lying quartet states and in which g_z values significantly larger than g_e can be easily accounted for.[27]

For a d_{z^2} ground state, the application of the model developed by McGarvey in conjunction with the approximation suggested by Raynor,[23] that uses a single (average) value for the energy of the quartet states, the following equations for the g tensor components are obtained

$$g_z = 2.0023 + 2C_3^2 + 3C_1C_2 - 3C_2^2 - 3C_1^2 \quad (1a)$$

$$g_x = 2.0023 + 2C_3^2 - 3C_1C_2 - 3C_1^2 + 6C_2 \quad (1b)$$

$$g_y = 2.0023 + 2C_3^2 - 3C_1C_2 - 3C_2^2 + 6C_1 \quad (1c)$$

where $C_1 = \xi/\Delta(^2B_1)$, $C_2 = \xi/\Delta(^2A_2)$, $C_3 = \xi/\Delta(^4B_2)$,$\Delta(^nT_i)$ is the energy difference between the ^nT_i state and the ground state ($^2A_1$) and ξ is the one-electron spin–orbit coupling constant.

The solutions of eq 1 obtained for $\{Ni(3,5\text{-}Cl_2saloph)\cdot[(CH_3)_2SO]_2\}^+$ are $C_1 = 0.031$, $C_2 = 0.036$, and $C_3 = 0.103$. The values of C_1 and C_2 yield approximate energies for the excited doublet states $^2A_2/^2B_1$ of ca. 11400/9900 cm^{-1}, assuming 50% reduction for the spin–orbit coupling, in reasonable agreement with the electronic spectra. The value of C_3, assuming the same reduction for the spin–orbit coupling, gives the (average) energy of the quartet states as 3500 cm^{-1} above the ground state, confirming their important contribution to the spin Hamiltonian parameters. For the adducts, the solution of eqs 1 yields values of C_3 in the range of 0.110/0.116, that imply an average energy for the quartet states of ≈3100–3250 cm^{-1} above the ground state, which, as expected, is lower than that observed for the complex ion the absence of axially coordinated bases, as expected. The observed values of C_1 are in the range 0.022–0.025 and those of C_2 are in the range 0.026–0.030 (Table III) and, assuming an orbital reduction of 50%, they are associated with $E_{xz,yz \rightarrow z^2}$ = 15900–14500 cm^{-1} and $E_{yz \rightarrow z^2}$ = 14000–12000 cm^{-1}. We did not observe this blue shift for the bands of the pyridine adducts, since the average lifetimes of the fluid solutions, prepared by the methods described, were not long enough to enable their spectral observation.

The reasonable inverse correlation observed between the values of $g_\perp$ of the adducts and the strength of the bases, as quantified by their proton affinities (Table I), can then be explained by strong σ bonding between the metal d_{z^2} and the axial pyridine lone pair orbital, thus destabilizing the semioccupied metal orbital (higher σ antibonding character). Taking the values of $^1/_2(g_x + g_y)$ as a good indication of $g_\perp$, and assuming that $C_1 \approx C_2 = C$ and neglecting second-order terms, $g_\perp$ is then given by

$$g_\perp \approx 2.0023 + 6C$$

where $C = \xi/\Delta$ and Δ is the difference in energy between d_{z^2} and $d_{xz} \approx d_{yz}$,[28] thus implying that an increase in Δ would result in a decrease in C and $g_\perp$. A remark concerning the axes labels has to be made, since no single-crystal data are available for nickel(III) complexes with N_2O_2 tetracoordinate equatorial bases and axial N donors. The use of the x and y labels cannot be interpreted as to suggest any preferential orientation of the plane of the axial coordinated bases, but nevertheless the results point toward a preferred orientation along the x or the y axis as represented in the drawing of compound **1**.

Nitrogen Superhyperfine Tensor and Spin Density on Axial Nitrogen Atoms. Because there is a direct interaction of the unpaired electron in the d_{z^2} nickel orbital with the axial nitrogen atoms of the pyridines, the signs of the experimental isotropic hyperfine tensor components and those of experimental values of $A_z(N)$, $A_x(N)$, and $A_y(N)$ will be positive. The anisotropic superhyperfine tensor was calculated after correction for indirect dipolar coupling using the point-dipolar approximation[30] assuming a value of 200 ppm for the Ni–N axial bond distance as observed in other Ni(III) complexes.[31]

The isotropic N coupling constants yield the 2s spin densities ($C_{2s}^2 = A_{iso}/A_s^{100}$; A_s^{100} = 557 G[30]) and the principal value of the anisotropic tensor (A_{zz}) gives the 2p spin densities ($C_{2p}^2 = A_{zz}^{corr}/A_p^{100}$; A_p^{100} = 33.5 G[30]) in the nitrogen atoms of the axial base. The 2s and 2p spin densities, the ratio p:s ($\lambda^2 = C_{2p}^2/C_{2s}^2$) and the total spin density delocalized onto the axially bounded pyridines are reported in Table IV.

Analysis of the data in Table IV shows that the calculated 2s, 2p, and total unpaired spin densities exhibit a linear dependence on the base strength (as measured by their proton affinities), with the 2s unpaired spin densities changing very little with the specific pyridine used (0.3%) when compared with the change in 2p spin densities (4%).

The 2s unpaired spin densities increase with the base strength, whereas the 2p spin densities decrease with an increase in base strength. This latter result can be interpreted as to suggest slightly longer Ni–N bond length for the weaker bases, since a larger p character in the lone pair directed to the metal, is expected to weaken the bond.[32] This explanation is consistent with the, already noted, linear decrease in $g_\perp$ with base strength, as shorter metal–base bond lengths will increase Δ.

The total spin density delocalized onto the nitrogen atoms shows a similar dependence on base strength as the 2p spin densities. The observation that spin density decreases with an increase in base strength can be interpreted as to imply that strong bases push spin density in the d_{z^2} orbital away from the metal and into the equatorial ligand. This could explain the fact that very strong bases do not stabilize Ni(III) complexes, but induce the formation of radical species (Table II). In fact, for the more basic substituted pyridines used, the only EPR spectra obtained were those characteristic of radical species.

Since there is a relationship between total spin density and base strength, it would be of interest to assess the transferability of linear free energy relationships, developed for organic chemistry, to our compounds. No analysis was performed for 2-substituted pyridines since steric effects could mask electronic contributions from the substituents. We used the dual substituent parameter (DSP) approach and tried to fit the data on an equation of the form

$$\Delta R = \rho_I\sigma_I + \rho_R\sigma_R^+ \quad (2)$$

where ΔR is the difference between the total spin density in coordinated pyridine and in the substituted pyridines, and σ_I and σ_R^+ have their usual meaning.[33,34] Two straight lines were observed (Figure 4) for the 3-substituted pyridines, $\Delta R = -5.16\sigma_I - 3.66\sigma_R^+$, with a correlation coefficient of 0.999, $f = 0.04$,[35] and $\rho_R/\rho_I = 0.71$, and for the 4-substituted pyridines, $\Delta R = 0.18\sigma_I + 8.68\sigma_R^+$, with a correlation coefficient of 1.000, $f = 0.02$, and $\rho_R/\rho_I = -48$.

(26) Maki, A. H.; Edelstein, N.; Davison, A.; Holm, R. H. *J. Am. Chem. Soc.* **1964**, *86*, 4580.
(27) McGarvey, B. R. *Can. J. Chem.* **1975**, *53*, 2498.
(28) McAuley, A. Morton, J. R.; Preston, K. F. *J. Am. Chem. Soc.* **1982**, *104*, 7561.
(29) Hitchman, M. A. *Inorg. Chim. Acta* **1977**, *26*, 237.
(30) Goodman, B. A.; Raynor, J. B. *Adv. Inorg. Chem. Radiochem.* **1970**, *13*, 135.
(31) (a) Yamashita, M.; Toriumi, K.; Ito, T. *Acta Crystallogr.* **1985**, *C41*, 1607. (b) Wieghardt, K.; Walz, W.; Nuber, B.; Weiss, J.; Ozarowski, A.; Stratmeier, H.; Reinen, D. *Inorg. Chem.* **1986**, *25*, 1650.
(32) Bent, H. A. *Chem. Rev.* **1961**, *61*, 275.
(33) Lowry, T. H.; Richardson, K. S. *Mechanism and Theory in Organic Chemistry*, 3rd ed.; Harper and Row: New York, 1987.
(34) *Correlation Analysis in Chemistry*; Chapman, N. B., Shorter, J., Eds.; Plenum: New York, 1978.
(35) The quantity f represents the "goodness of fit" of the data to eq 2; f test values less than 0.1 indicate an excellent fit and those between 0.1 and 0.2 an acceptable fit. See Arnold, D. P.; Bennett, M. A. *Inorg. Chem.* **1984**, *23*, 2117.

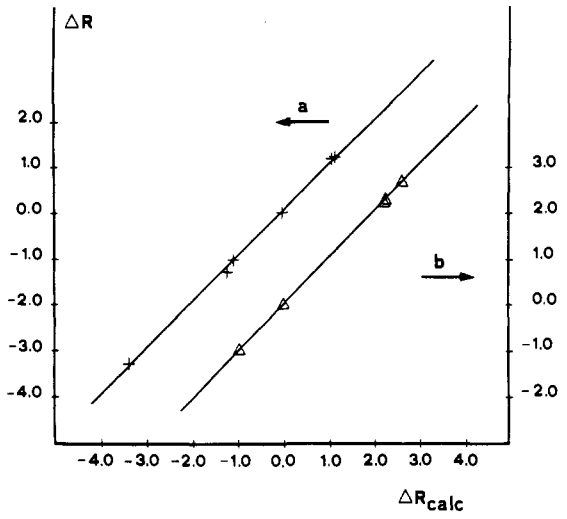

Figure 4. Plots of measured values of ΔR (spin densities differences) for $[Ni(3,5\text{-}Cl_2saloph)\cdot B_2]^+$ vs values calculated with the following relationships: (a) for 3-substituted pyridines $\Delta R = -5.16\sigma_I - 3.66\sigma_R^+$; (b) for 4-substituted pyridines $\Delta R = 0.18\sigma_I - 8.68\sigma_R^+$.

Application of the DSP treatment to the proton affinities, gives, for the same meta substituents, the following values: $\Delta PA = 73.08\sigma_I + 29.86\sigma_R^+$, with a correlation coefficient 0.994, $f = 0.09$, and $\rho_R/\rho_I = 0.41$, whereas for the same para substituents $\Delta PA = 58.30\sigma_I + 67.44\sigma_R^+$, with a correlation coefficient 0.994, $f = 0.15$, and $\rho_R/\rho_I = 1.16$.

For the 3-substituted pyridines, the similar values obtained for the ratio ρ_R/ρ_I indicate that inductive and resonance effects are of similar magnitude in the proton affinities and in the unpaired spin densities. For 4-substituted pyridines, the very large value of ρ_R/ρ_I obtained from the unpaired spin density analysis indicates a major contribution from resonance (π ring) effects and an almost negligible contribution of inductive effects, and contrasts with values of ρ_R and ρ_I of the same order of magnitude from the proton affinity analysis. The striking difference in ρ_R/ρ_I for the 4-substituted pyridines suggests different effects in the proton and the metal cases. A possible explanation would involve a π interaction between the pyridine ring and metal d orbitals, thus making π effects being dominant in the substituent contribution at the N pyridine atom, but our data are not sufficient to establish any more detailed a model.

Concluding Remarks

The oxidation of nickel(II) bis(salicylaldiimine) complexes in weak donor solvents was shown to proceed through oxidation of the equatorial ligand immediately followed by radical polymerization.[5] On the other hand, we have shown that in strong donor solvents (DN higher than 14), the oxidation of the Ni(II) complex of bis(3,5-dichlorosalicylaldehyde) *o*-phenylenediimine takes place at the metal center, and EPR spectra characteristic of d^7 metal complexes were obtained. In the presence of pyridines with PA lower than ~945 kJ mol^{-1}, the solvent molecules are replaced by the bases and new species, formulated as $[Ni(3,5\text{-}Cl_2saloph)\cdot B_2]^+$, are present in solution as can be inferred from the superhyperfine coupling with axial nitrogen atoms in the EPR spectra. However, the stronger pyridines (PA greater than ~945 kJ mol^{-1}) the metal oxidized species rapidly and irreversibly decompose into radical intermediates that are spectroscopically detectable and so prevent, under the experimental conditions used, the observation of spectra characteristic of Ni(III) compounds.

For the oxidation to take place at the metal center in nickel(II) bis(salicylaldiimine) complexes, the presence of moderately strong bases coordinated axially is necessary. This suggests that the ratio between equatorial/axial ligand fields must play a decisive role in the stabilization of the +3 formal oxidation state in the metal. For each equatorial ligand, there must exist an interval of axial base strength, for which the unpaired electron will be essentially localized in a metal orbital. Such a fine tuning in the balance between metal/ligand oxidation sites for these complexes suggests that small changes in the equatorial ligand, via electron withdrawing/donating groups, can appreciably change the overall stability of Ni(III) species and the range of bases that stabilize them. Studies with other similar ligands are in progress.

EPR spectroscopy has proved to be the technique of choice in the study and characterization of the molecular geometry of Ni(III) compounds and in the study of the influence of ligand donor character on electron delocalization within the metal–ligand bond. The application of McGarvey's model for d^7 low-spin systems, successfully interprets the spin Hamiltonian parameters of Ni(III) and also accounts for the large g_z values observed in terms of mixing of the low lying excited quartet states with the ground state. Spin density on the metal was not calculated, since $I = 0$ for ^{58}Ni and ^{60}Ni, but extension of the proposed analysis to an isotopically enriched nickel compound would provide further tests for the model and also allow an estimate to be made of the unpaired spin density in the metal, and consequently in the equatorial ligand.

Finally, the application of the concepts developed in physical organic chemistry, to account for the electron density in the metal center and to assess the mechanisms of unpaired spin density transfer to the axially coordinate bases, looks promising, despite the limited data set used in this study. The utility and limitations of the method require further work.

Acknowledgment. This work was supported by Instituto Nacional de Investigação Científica (INIC, Lisboa) through Contract No. 89/EXA/3. C.F. thanks INIC for a fellowship. Thanks are due to CIQ(UP) Linha 7 for use of their cyclic voltammetry equipment and to C. Moura for assistance with the electrochemical measurements.